جامعة الانبار

كلية العلوم -قسم الجيولوجيا التطبيقية

اسم المحاضر باللغة الانكليزية: **Ali Mishaal Abed**

اسم المحاضر باللغة العربية: علي مشعل عبد

اسم المادة بالإنكليزي: **Electrical Methods**

اسم المادة بالعربي: الطرق الكهربائية

عنوان المحاضرة بالإنكليزي: **Measuring techniques**

Measuring techniques

Three categories of field techniques exist for conventional resistivity analysis of the subsurface. These techniques are: constant separation traversing (CST), vertical electric sounding (VES), and Combined VES/CST surveys.

Constant Separation Traversing (CST)

Horizontal profiling

Electrical profiling uses collinear arrays to determine lateral resistivity variations in the shallow subsurface at a more or less fixed depth of investigation. The current and potential electrodes are moved along a profile with constant spacing between electrodes. Maximum apparent resistivity anomalies are obtained by orienting the profiles at right angles to the strike of the geologic structure. The obtained values of apparent resistivity from horizontal profiling are interpreted qualitatively by plotting apparent resistivity profiles, where the geometric center of the electrode array at the abscissa and the apparent resistivity at the ordinate.

In certain survey, a method of horizontal profiling called Schlumberger $\overline{AB}$ profiling or sometimes called Brant array. In this technique the two current electrodes may be placed a large distance apart and the potential electrodes moved along the middle third of the line $\overline{AB}$ (Kunetz, 1966) as in figure (2.10).

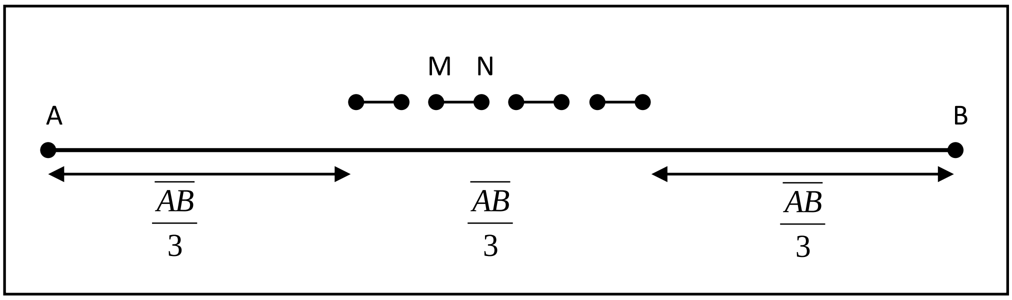

Figure (2.10) Electrodes array for Schlumberger AB profile, also called Brant array.

Lateral resistivity mapping

Resistivity mapping (generally) depends on the horizontal profiling technique because it is taken along a series of parallel traverses, when one traverse is finished, the array is moved to the next parallel line and so forth until the area of investigation is covered, the apparent resistivity of the center point of each spread can be plotted on a map and equi-resistivity contours can be drawn. This equi-resistivity map has a failing according to (Van Nostrand and Cook, 1966); although this map forms a very effective picture of the progress of the survey if it is kept current.

A modification of the Schlumberger $\overline{AB}$ profile procedure where the potential electrodes are moved not only along the middle third of the line $\overline{AB}$ but also along lines laterally displaced from and parallel to $\overline{AB}$ (where the lateral displacement may be as much as $\frac{\overline{AB}}{4}$) is called the Rectangle of Resistivity method (Kunetz, 1966) as in figure (2.11).

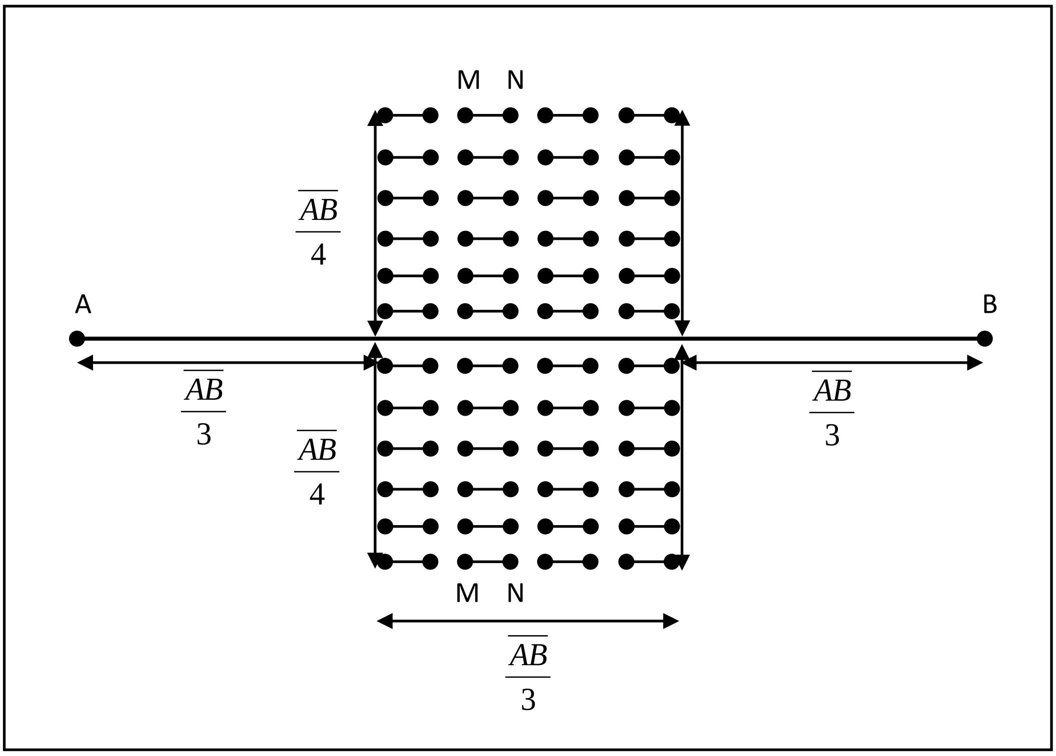

Figure (2.11) Electrodes array for Rectangle of Resistivity Method.

Another mapping technique called Line-electrode survey as in figure (2.12) (Parasnis, 1965). At this technique each electrode consists of a long bar copper wire which is tightly looped every 5-10m around a long iron nail this being pegged into the ground. The two electrodes are parallel to each other and a few hundred to several hundred meters long. The current electrodes are laid parallel to the geological strike.

Each electrode is connected to one pole of a DC generator. The connection is made at (at least) two points of the electrode on either side of its centre.

A measurement consists in reading the voltage difference between a pair of potential probes placed on a line perpendicular to the current electrodes. The distance between the probes is small compared with the distance between the current electrodes and measurements are not made nearly to either current electrode.

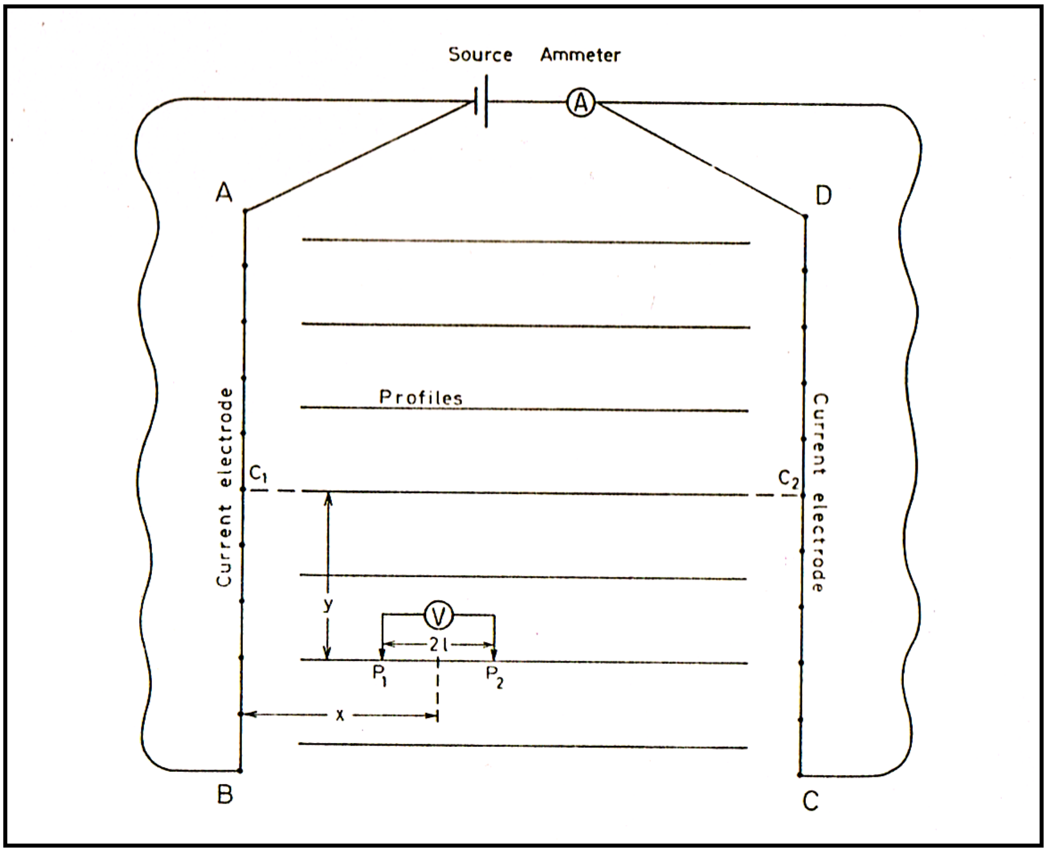

(2.12) Layout for line electrode surveys.

The interval between the observation points is usually 40m for reconnaissance survey and 10-20m for detailed ones. Lines are spaced 40 or 20m apart and measure in a zigzag manner until the area is covered.

This technique was used for: a) outcropping vertical contact between two extensive rock formations, b) outcropping vertical vein with the rocks on either side differing in resistivity from each other and from the vein, c) outcropping dipping contact, d) semi-circular trough flush with the earth's surface and e) horizontally stratified earth.

The measurement can be represented as maps show the two-dimensional distribution apparent resistivity.

Azimuthal Resistivity Survey

The first aim of resistivity survey is a study of any inhomogeneities. Frequently in practice, the effect of anisotropy is displayed together with that of layering or inhomogeneities. It complicates data interpretation within the framework of anisotropic models, and distorts results of interpretation in the framework of layered or inhomogeneous media. At the same time anisotropy studying can give valuable geological information. On definition, rock anisotropy is displayed in apparent resistivity values as dependence on array orientation and as independence on coordinates. Azimuthal (or circular) resistivity survey (ARS) is the best field technology for anisotropy studying.

- **Type of array rotation in azimuthal resistivity survey**

In azimuthal resistivity survey, there are two types of array rotation:

1- Symmetrical azimuthal resistivity survey

This survey is conducted using the same array spacing and with the center of the spread on the same position (figure (2.13)). Each successive spread is oriented in a different direction or azimuth until 180 degrees are covered in increments of 30 degrees. A full 360 degrees need not be surveyed at the setup for 0 degrees gives the same result as for 180 degrees and 30 degrees the same result as 210 degrees, etc.

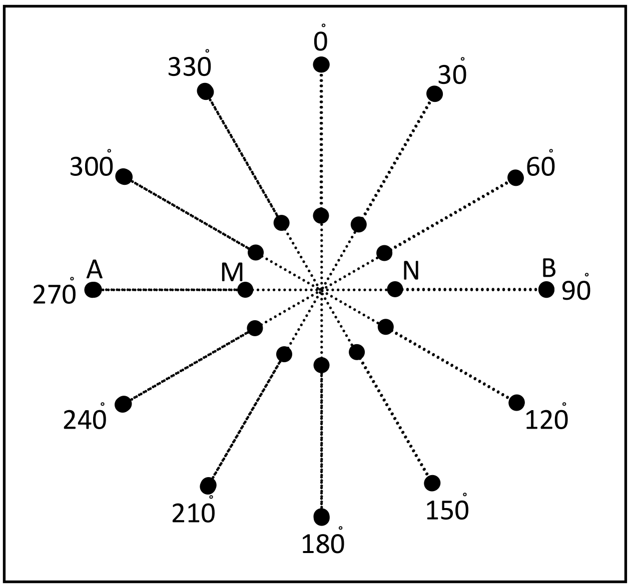

Figure (2.13) Layout of symmetrical azimuthal resistivity survey. A Wenner array is rotated 30 degrees clockwise.

2- Non-symmetrical azimuthal resistivity survey

This survey is conducted using the same array spacing, but the centre of array is changed with changing the all spread direction. This survey can be done with two layouts: At the first layout, the position of all the four electrodes changing as in figure (2.14a). At the second layout, one of the current electrodes keeps fixed while the other electrodes move out to next positions at a new direction as in figure (2.14b).

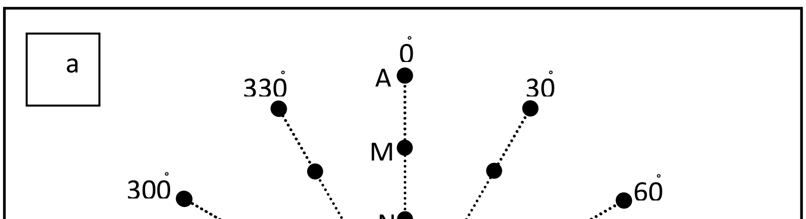

Figure (2.14) Layout of non-symmetrical azimuthal resistivity survey. a) The position of all the four electrodes moved out. b) One of the current electrodes keeping fixed.

- **Data visualization in azimuthal resistivity survey**

There are several ways in which azimuthal resistivity data may be displayed so that one or another aspect of the data may be emphasized.

Nunn *et al.* (1983) plotted resistivity data as a function of azimuth in Cartesian coordinates as in figure (2.15).

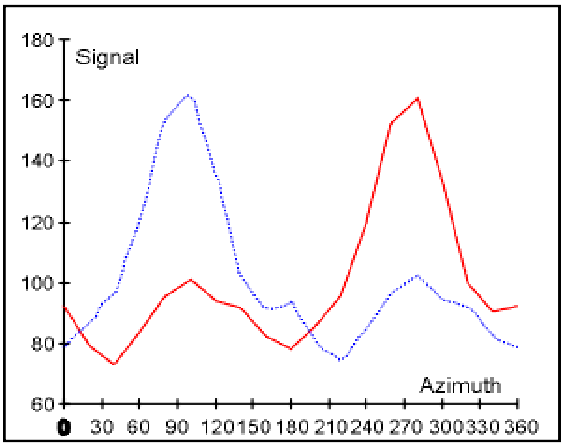

Figure (2.15) Azimuthal resistivity diagram in Cartesian coordinate from (Nunn *et al.*, 1983).

The most common form of data presentation is through polar coordinates, where apparent resistivity values are plotted along definite azimuth, where any point plotted at a distance from the diagram's center along the same azimuth with definite linear scale. All points are connected with a curve as in figure (2.16) (Taylor and Fleming, 1988).

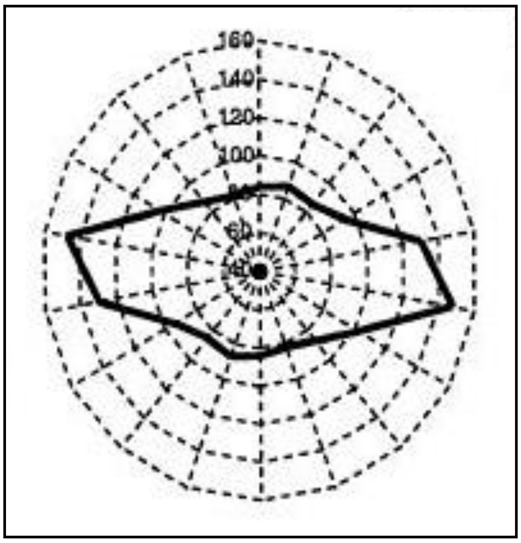

Figure (2.16) Azimuthal resistivity measurements in polar coordinates from (Taylor and Fleming, 1988).

- **Analyzing azimuthal resistivity data**

Azimuthal resistivity surveys are performed to determine the direction of anisotropy in soils or rock.

Steinich *et al.* (1997) calculated the anisotropy (λ) from the ratio between the largest apparent resistivity (ρ_a max) and the smallest apparent resistivity (ρ_a min) in the azimuthal resistivity curve as:

$$\lambda = \frac{\rho_a \max}{\rho_a \min} \quad ..... (21)$$

Thus the value of (1) for (λ) is an index characterizing the eccentricity of the curve with respect to a circle, which would be expected for an isotropic medium and for which the value of 1 would be unity.

Another measure determines if azimuthal variations indicate anisotropy, which allows discrimination in the data between an elliptical azimuthal response model indicative of anisotropy or a circular azimuthal model indicative of isotropy. R^2 is the percentage of variance, σ^2, from the circular curve, which has been removed by the elliptical curve and is expressed with the equation (Busby, 2000):

$$R^2 = \frac{\left(\sigma^2{}_{(circle)} - \sigma^2{}_{(ellipse)}\right)}{\sigma^2{}_{(ellipse)}} \ldots\ldots (22)$$

A perfectly anisotropic model has an R^2 value of 1, where low values around 0.2 indicate an isotropic model.

Also another measure of anisotropy is used to describe the orientation of the ellipse by determining the strike azimuth of the major axis of the ellipse. Quantitative measures of anisotropy include percentage variation about the average is:

$$\pm 0.5\left[\frac{(\rho_{\max} - \rho_{\min})}{\rho_{average}}\right]100\% \ldots\ldots (23)$$

Vertical electrical sounding (VES)

Electrical resistivity sounding has been in use since 1913 and went through major developments during the 1980s. VES is designed to provide vertical profiles of resistivity versus depth. This technique is based on the general observation that current penetrates deeper into the subsurface with increasing separation of electrodes.

In an electrical sounding the electrode array is systematically made larger while the center of the array remains fixed over the area of interest. As the array gets larger, the electric currents flowing deeper and deeper in the earth are sensed, and so the resistivity of deeper and deeper structure is measured.

In a Schlumberger array the M and N electrode array is held fixed while the A and B current electrodes are moved outward by constant lengths. This movement signifies an increased depth of measurement as the current electrodes are moved farther apart. When the current electrodes are moved apart, the potential recorded from the M and N electrodes ΔV becomes smaller and ultimately becomes too small to measure. At this point, the potential electrodes are moved out and measurements continue change as the current passes through different rock. At a certain point, depending on the sample area, the MN potential will fall below the accuracy of the voltmeter in use.

Schlumberger array is the most favorable array for VES because:

1. The measured apparent resistivity is more representative to the center of array (Al-Ani, 1998 in arabic).
2. For the theoretical case, the measured apparent resistivity is more representative to the depth function because the four components of apparent resistivity (ρ_{AM}, $\rho_{AN,}$ ρ_{BM} and ρ_{BN}) are approached (Al-Ani, 1998 in arabic).

An individual data set contains data from one pair of potential electrodes in the array, and apparent resistivity curve is made from each electrode pair. It is plotted as (ρ_a) vs. (AB/2). So each time the distance AB increases, each electrode pair gives an additional data point to graph on the resistivity curve. In the resistivity curve both the resistivity and spacing scales being logarithmic. Logarithmic scales are used because: a) the range in resistivity of earth materials is more than 5 orders of magnitude and b) the resistivity method is only sensitive to structure which is of comparable size to its depth of burial.

One of the most important steps in interpretation is curve smoothing process because the interpretation is based on the final shape of the curve which is related to smoothing procedure. Usually, the field curve suffered from distortion. There are several kinds of distortion described by Zohdy *et al.* (1974). Here we will focus on one type which is the most important and most common (in the field curves of this study), which is the displacement in field curve segments.

Schlumberger field curve suffers from two kinds of displacement:

1- Vertical displacement:

This displacement occurs at the repeated measurements when we fixed the distance ($\overline{AB}$) and increase the distance ($\overline{MN}$).

This displacement is caused by two reasons:

a) Theoretical errors:

Al-Ani (1998 in arabic) show that these displacements in the repeated measurements occur because of getting two different values of (ρ_a), each value comes from different apparent depth. This displacement differs according to the ratio ($\frac{\overline{MN}}{\overline{AB}}$). By increasing the distance ($\overline{MN}$), the displacement between the field curve and the theoretical curve, which depends on the ratio ($\frac{\overline{MN}}{\overline{AB}}$), increase.

The Schlumberger curve then can be rectified and smoothed according to (Zohdy, 1974) as shown in figure (2.17).

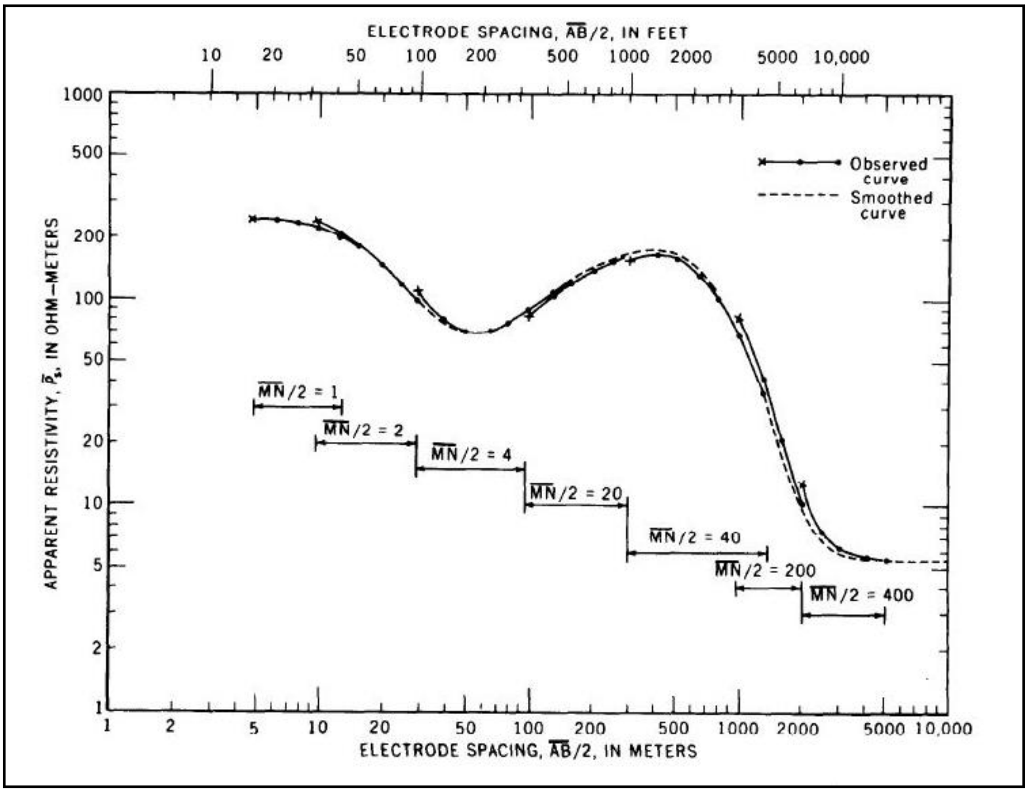

Figure (2.17) Correct displacement on a Schlumberger sounding curve and method of smoothing from (Zohdy *et al.,* 1974).

Al-Ani (1998) pointed out that this displacement must occur because in the field the distance ($\overline{MN}$) is greater than zero, so decreasing this displacement as possible is better than making correction to the field curve, and that through keeping the ratio ($\frac{\overline{MN}}{\overline{AB}}$) ranging between ($\frac{1}{5}-\frac{1}{12}$), and furthering ($\overline{MN}$) distance while fixing ($\overline{AB}$) distance during measurements is better to be more than ($2.5\overline{MN}$).

b) Near surface inhomogeneities (NSI):

Difference between NSI and deep objects depends on our selection. Some bodies in definite depth interval is considered as useful objects and adjust field technology for their tracing, while some others on smaller depth we consider as noise. Distortions of the electric field (or VES curves), caused by such NSI objects may be divided into two principal types: caused by object near dipole element of array and caused by object near single electrode. These effects depend also on the fact: is this dipole group or single electrode moveable or unmovable.

Bobachev *et al.* (1997) used more local terms to classify distortions which are related to (NSI):

1. **P-effect:** was named from the word "potential". P-effect shows itself as a vertical shift of VES curve along axis ρ_a without form changes. The main cause of P-effect seems to consider $\rho_{a\ MN}$ at the location of NSI. If VES curve is non-segmented, that P-effect may be found in comparison of this curve with the neighbors. For segmented curve P-effect gives the shift of segments for different MN with the total form of curve being conserved as in figure (2.18).

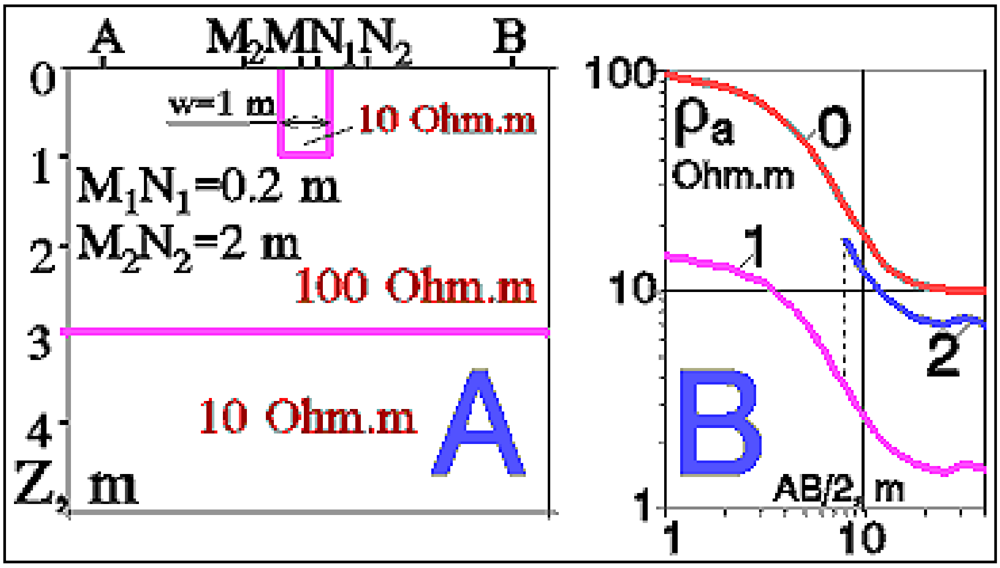

Figure (2.18) P-effect on segmented VES curve. A) model and B) VES curves.

P-effect removing is called normalization. For segmented curve it may be done firstly by partial normalization (all segments are moved up to coming into contact with each other) and then by fuller normalization (all VES curves on profile are moved to the same base level of apparent resistivity). This base level may be selected on the most unchangeable part of all curves as in figure (2.19).

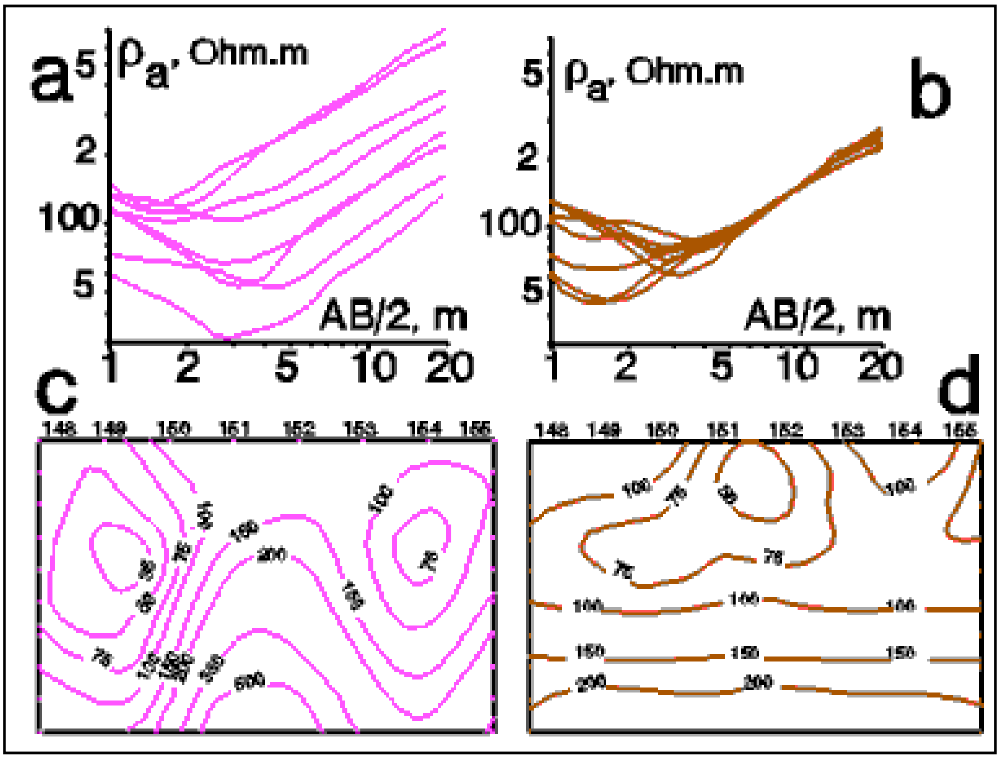

Figure (2.19) P-effect on field VES data.

As a result of P-effect, apparent resistivity pseudo-section looks like wavered structure [figure (2.19, c)]. Step between VES sites in figure (2.19) is equal to 1 meter with maximal Ao distance being equal to 20 m. That means that differences between VES curves resulted from distortions, and not from real deep structure. After moving all VES curves to one ρ_a level [(figure (2.19, b)], apparent resistivity pseudo-section became horizontal [(figure (2.19, d)] and interpretation gives horizontal boundaries.

2. **C-effect**: was found and described in 1991, firstly in modeling results and only after that in field data. The main cause of that is in the difficulty of finding C-effect on (ρ_a) pseudo-cross-section when all VES's were measured with logarithmic distance step. On figure (2.20) is shown results of modeling VES over two-layered structure with one NSI. [a) - the model, b) - NSI and c) - different VES curves for several variants of meeting elements of array], (0 non-distorted and 1-4 distorted by P or C-effect). Some distortions of sounding curves are conformable [figure (2.20c, 1-2)], whereas others are non conformable [figure (2.20c, 3-4)]. When moving current electrode hits the NSI, VES curve noticeably changes on one or two distances due to abrupt change in current density in the cross-section.

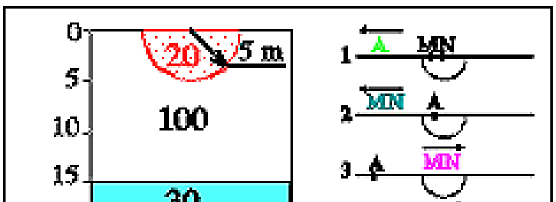

Figure (2.20) Shows results of modeling VES over two-layered structure with one NSI

2- Horizontal displacement:

The maximum change in apparent resistivity always occurs at an electrode spacing that is larger than the depth at which the corresponding change in true resistivity occurs. That is, a sounding curve is "out of phase" with the resistivity-depth curve and is always shifted to the right of the resistivity-depth curve (Zohdy, 1989).

That means, all the measured values at every part of the field curve parts (including the repeated measurements) include horizontal displacement because of the difference between the depth of investigation and the depth function ($\frac{\overline{AB}}{2}$). This displacement is always to the right because the depth of investigation is always less than the depth function.

So, for interpretation, Zohdy (1989) found that the sounding curve must be shifted to the left in order to be in phase with resistivity-depth curve by multiplying all the electrodes spacing by fixed depth shift factor, and he found that each sounding curve has its unique depth shift factor. The value of this sift factor depends on:

a) Curve type.

b) The completeness of the left and right branches of the field curve.

c) The amount of noise present.

He found that, a fixed shift factor may be selected from the range between 0.3 and 0.6 (approximately) and used for almost all Schlumberger curve types.
Using a fixed shift factor by Zohdy for depth correction for Schlumberger array is incorrect because Al-Ani (1998) concluded that there are many depth functions for this array which depend on the difference between the apparent depth of minimum operating distance and the apparent depth of mean operating distance, and this difference changes according to change the ratio ($\frac{\overline{MN}}{\overline{AB}}$). So according to the conclusion Al-Ani, there must be more than one depth shift factor, one for every investigated depth.

Combined VES/CST Surveys

Combined VES/CST surveys offer the most information. As with CST alone, multiple VES/CST surveys can be planned in order to characterize (image) the vertical as well as horizontal extent of subsurface variations. Images of the subsurface are called pseudo-sections because data measurements with respect to depth are only simply represented.

DC resistivity imaging techniques

In practice, the arrays that are most commonly used for 2-D imaging surveys are the (a) Wenner, (b) dipole-dipole (c) Wenner- Schlumberger (d) pole-pole and (e) pole-dipole. These arrays are commonly used in resistivity surveys. They have their strengths and their weaknesses. They are typically described by their signal-to-noise ratio, their depth of investigation, their ability for lateral location of the target and their mapping abilities of horizontal layers or steeply dipping structures among other factors (Ward 1990).
We shall concentrate on Wenner array because it will be used in this study. In figure (2.21), the sensitivity plot for the Wenner array has almost horizontal contours beneath the center of the array. Because of this property:

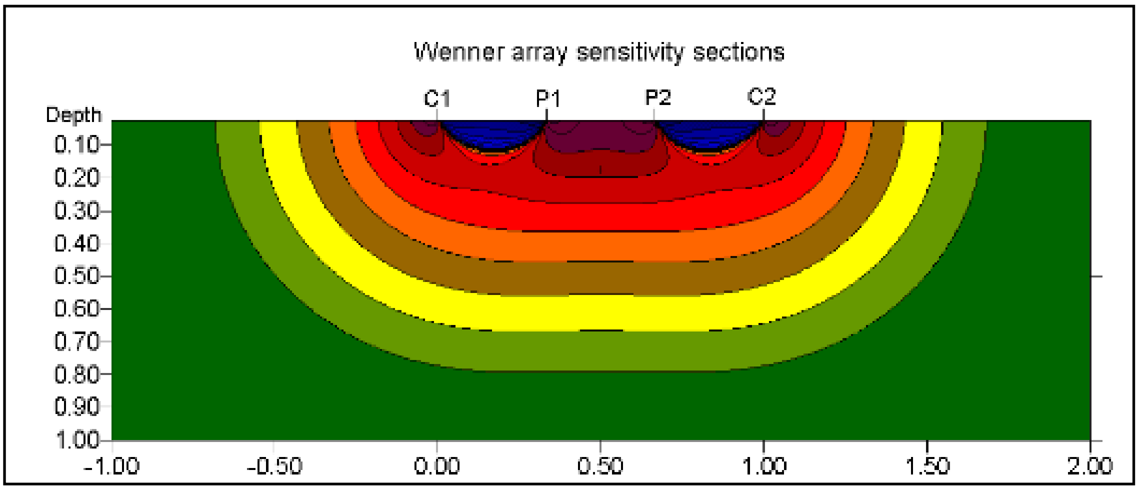

Figure (2.21) 2-D sensitivity sections for the Wenner array.

1. The Wenner array is relatively sensitive to vertical changes in the subsurface resistivity below the center of the array. However, it is less sensitive to horizontal changes in the subsurface resistivity (Dahlin and Zhou, 2004).
2. In general, the Wenner array is good in resolving vertical changes (i.e. horizontal structures), but relatively poor in detecting horizontal changes (i.e. narrow vertical structures).
3. The median depth of investigation for the Wenner array is approximately 0.5 times the “a” spacing used. Compared to other arrays, the Wenner array has a moderate depth of investigation (Edwards, 1977).
4. The geometric factor for the Wenner array is ($2\pi a$). This is smaller than the geometric factor for other arrays. Among the common arrays, the Wenner array has the strongest signal strength because the signal strength is inversely proportional to the geometric factor used to calculate the apparent resistivity value for the array. This can be an important factor if the survey is carried in areas with high background noise.
5. One disadvantage of this array for 2-D surveys is the relatively poor horizontal coverage as the electrode spacing is increased. This could be a problem if you use a system with a relatively small number of electrodes.

Data collection

Data acquisition was almost uniquely carried out manually till the 1980s. The four electrodes were placed in the ground and moved manually, between each data point measured, which is labor intensive and slow. Thus imaging was limited to either mapping the variation of apparent resistivity over a surface using one or a few different electrode separation(s), or compiling quasi - 2D sections from a rather limited number of VES.

Use of multi – electrode systems for the data acquisition allows a dramatic increase in field productivity so that one person rather than three can conveniently carry out sounding with limited layout. At first, systems with manual switching appeared (Barker, 1981), and eventually the computer – controlled system with automatic measurement and data quality control (Dahlin, 1989) which demands the use of automated multi-electrode data acquisition system to be practical.

1) 2D Imaging mode

To obtain a good 2-D image of the subsurface, the coverage of the measurements must be 2-D as well. As an example, figure (2.22) shows a possible sequence of measurements for the Wenner electrode array for a system with 20 electrodes.

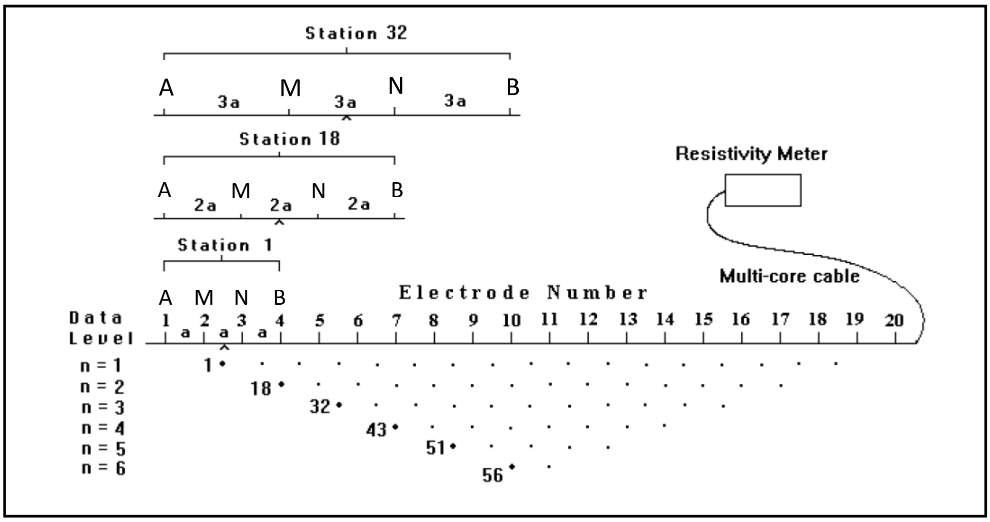

Figure (2.22) The arrangement of electrodes for a 2-D electrical survey and the sequence of measurements used to build up a pseudosection modified from (Barker, 1992).

In this example, the spacing between adjacent electrodes is “a”. The first step is to make all the possible measurements with the Wenner array with an electrode spacing of “1a”. For the first measurement, electrodes number 1, 2, 3 and 4 are used. Notice that electrode 1 is used as the first current electrode (A), electrode 2 as the first potential electrode (M), electrode 3 as the second potential electrode (N) and electrode 4 as the second current electrode (B). For the second measurement, electrodes number 2, 3, 4 and 5 are used for (A), (M), (N) and (B) respectively.

This is repeated down the line of electrodes until electrodes 17, 18, 19 and 20 are used for the last measurement with “1a” spacing. For a system with 20 electrodes, note that there are 17 (20 - 3) possible measurements with “1a” spacing for the Wenner array.

After completing the sequence of measurements with “1a” spacing, the next sequence of measurements with “2a” electrode spacing is made. First electrodes 1, 3, 5 and 7 are used for the first measurement. The electrodes are chosen so that the spacing between adjacent electrodes is “2a”. For the second measurement, electrodes 2, 4, 6 and 8 are used. This process is repeated down the line until electrodes 14, 16, 18 and 20 are used for the last measurement with spacing “2a”. For a system with 20 electrodes, note that there are 14 (20 - 2x3) possible measurements with “2a” spacing.

The same process is repeated for measurements with “3a”, “4a”, “5a” and “6a” spacings. To get the best results, the measurements in a field survey should be carried out in a systematic manner so that, as far as possible, all the possible measurements are made.

One technique used to extend horizontally the area covered by the survey, particularly for a system with a limited number of electrodes, is the roll-along method. After completing the sequence of measurements, the cable is moved past one end of the line by several unit electrode spacings, after which the data acquisition software automatically checks the electrode contact and scans through a pre-defined measurement protocol and new measurements are added. Measurements that involve the electrodes on part of the cable that do not overlap the original end of the survey line are repeated as in figure (2.23).

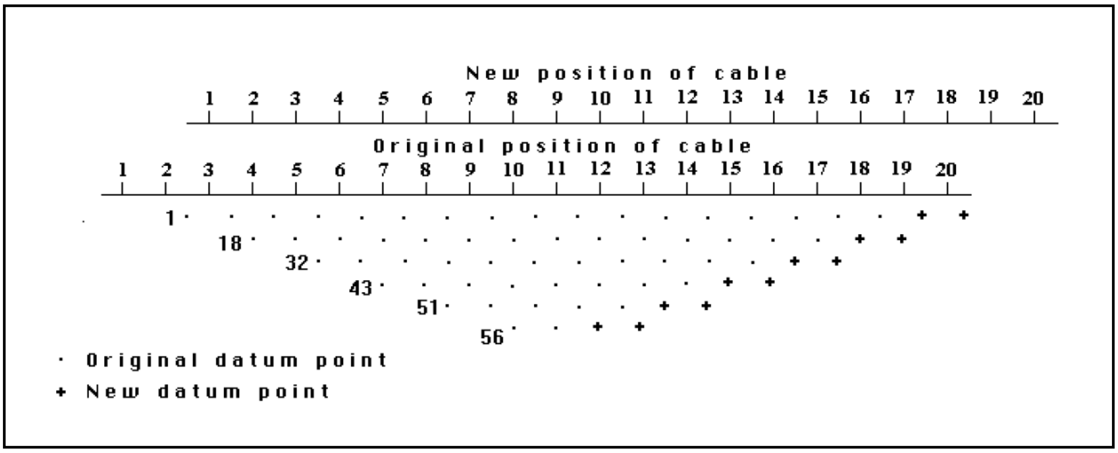

2) 3D imaging mode

3D measuring mode which involves laying out a number of electrodes on a 3D grid and measure a large number 4-electrode combinations in order to obtain information about the 3D variation of the subsurface resistivity. Practical field techniques were described by Loke and Barker (1996a). The initial suggestion involved the deployment of one multicore cable in snake-lines across a regular grid of electrodes as in

Figure (2.23) Practical the roll-alo

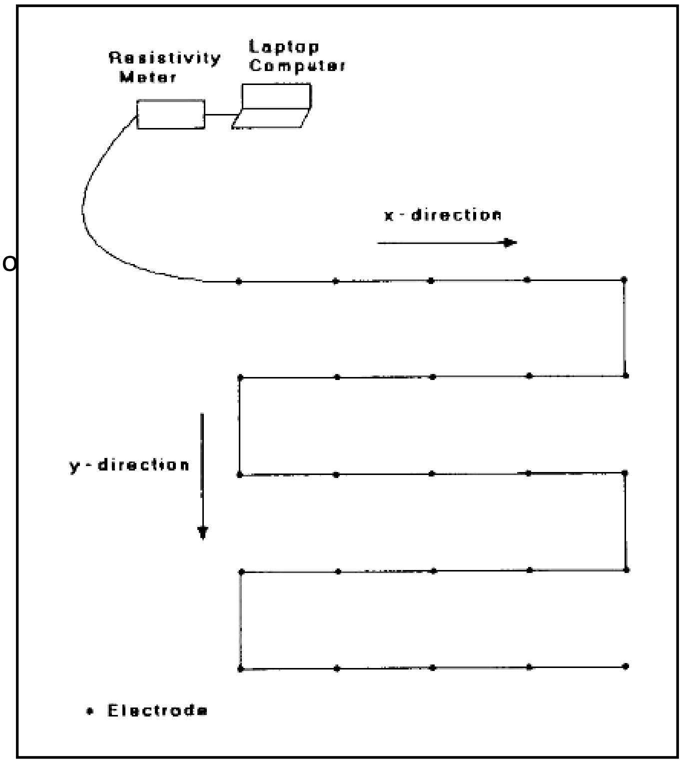

figure (2.24). However, such a procedure is only viable for small grids of the order of 10 × 10 electrodes. For larger (or more detailed) 3D surveys, data are usually acquired along a sequence of parallel lines which involves the installation of multiple cables or the use of roll-along techniques (Dahlin and Bernstone, 1997) in order to increase efficiency.

Figure (2.24) 3D measuring mode.

3D measuring mode treats successfully 3D structures; however it is expensive since it involves increased instrumentation (cable) and computational cost if data are to be treated with 3D inversion programs. The later is not an important problem considering the high increase in computer power but hardware logistics is most of the times prohibitive in measuring with the 3D mode particularly with large electrode spacing. So in practice instead of using the 3D measurement mode 3D resistivity variations are recorded by recording a dense 2D measurement grid which is considered to be a more practical and economical approach for field-data. Dense 2D sets involve measuring parallel 2D lines with inter-line spacing equal to the inter-electrode spacing. Measurements can take place along the X-axis (X-lines) [figure (2.25a)], or along the Y-axis (Y-lines) [(figure (2.25b), or along both axes (XY-lines) as depicted in figure (2.25c) (Tsourlos, 2004).
These dense 2D measurements are routinely being interpreted with 2D algorithms and the results are combined a-posteriori to generate pseudo-3D (x,y,z) images.

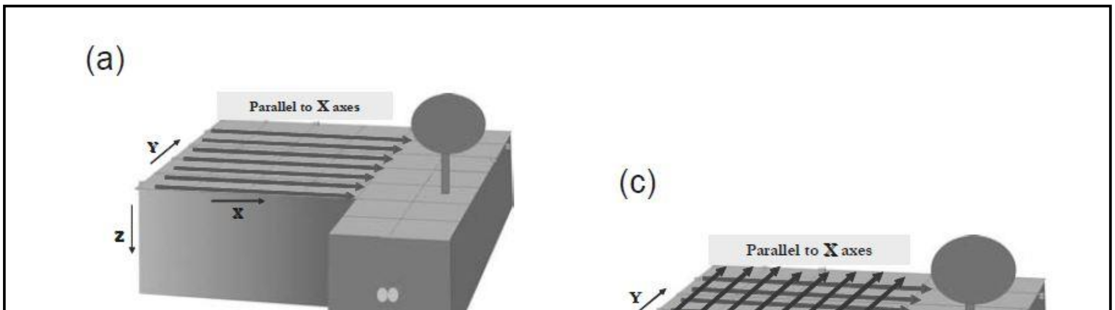

Figure (2.25) Dense 2D measurements. a) parallel to the X-axis (X-lines), b) parallel to the Y-axis (Y-lines) and c) combined XY-lines from (Tsourlos, 2004) .

This approach of combining dense 2-D measurement with 3D inversion is considered practical for routine data treatment since the extra computational time/power required by 3D inversion schemes is compensated by the reduced amount (50% less) of field data required when compared with the 2D approach (Tsourlos, 2004).

Measurement errors

To apply the imaging technique successfully, great attention must be paid to controlling the observed data quality in fieldwork and data processing, and any possibilities of minimizing the effects from all kind of error sources must be taken. For this reason it is important to investigate the properties of the data observation errors and understand their effect on the imaging results.
The Measurement errors may be simply classified into two kinds (Zhou and Dahlin, 2003):

1- Electrode spacing errors

The electrode spacing errors are caused by the measurement errors in electrode positions or inadvertent electrode setting up. In most cases of 2D resistivity imaging surveying multi-electrode cable with fixed spacing is employed along a measurement line. However, it is not uncommon that some portion of the cable cannot be straightened due to rough terrain or vegetation, or the positions are shifted to improve electrode contact with the ground. Sometimes the electrode positions are measured with a string or tape, with the associated risk of electrode spacing error due to human factor. In a practical situation one specific electrode array is normally chosen, such as the pole-pole, pole-dipole, Wenner or Schlumberger array. The magnitude of the spacing errors are quite different with these arrays, being largest for dipole-dipole, Wenner-β and γ, for which a 10% in-line spacing error may cause twice as large an error (>20%) in the observed apparent resistivity, which in turn will produce some artifact in the inverted model.

Szalai *et al*. (2007) proved that the noises of positioning origin are relatively low among even very inconvenient field conditions, and they have influenced only the near-surface data, and in order to be able to eliminate the problem of spacing errors they advised:

1) Avoid area where the surface rockiness is important (if it is possible at all).
2) Try to keep $|x_{ideal}-x_{real}|$ on minimum.
3) If we have only a few electrodes with wrong position, it is possible to ignore them and carry out the inversion without these data.
4) Taking into account the real position of the electrodes.

At the same time, as for the consequences on numerical modeling one should know the following:

1) The consequences of the positioning error on the pseudosection of apparent and inverted resistivities depend very much on the array geometry (the increasing order of these effects is: pole-pole, Wenner-α, pole-dipole, Wenner-β).
2) The error propagates systematically and not randomly.

Consequently in the inverted resistivity images the size of the false anomalies can be large.

2- The potential error

This error arises from many sources, such as bad electrode contact, cable insulation damage, site background noise (telluric current and power line noise), instrumental problems (the wrong current injection and picking - up of noise potentials) and improper instrument operation.

The data quality, or the observed potential error, may be estimated by normal and reciprocal measurements. Such data can be acquired efficiently using an automatic data acquisition system for all data points, although at the visualization algorithmic plot and the error pseudosection of the absolute relative errors calculated by the normal and reciprocal potential readings are very useful for quantitative and spatial evaluation of the data quality, which may be characterized by the mean value, standard deviation, regression function and the spatial distribution of the possible observed outliers.

The potential error increases as a power with the decrease in the measured potential, which reaffirms the fact that potential error depends on the strength of the measured signal and varies with sites, times and electrode configurations. Wenner, pole-pole and Schlumberger measurements have relative stronger potential signal than dipole-dipole and pole-dipole arrays.

The robust inversion and smoothness constrained least squares inversion can be applied to the assessment of real observed potential outliers and data quality of the normal surveying data. The smoothness constrained least squares inversion is sensitive to outliers in the data, which may produce artifacts or distorted in the inverted model. The robust inversion is fairly in sensitive to the outliers of data, and with high data quality the two inversion schemes produce very similar images except that obtained with the robust inversion is more "blocky" and has a slightly better data misfit.

Data processing

The measured apparent resistivities are then presented in a contoured pseudosection, A pseudosection is a display technique devised by Hallof (1957) which involves plotting resistivity traverse data as a depth section, with each apparent resistivity being plotted as if it were the true resistivity of a point immediately below the centre of the electrode array at a depth proportional to the electrode spacing. The contoured data provide an approximate picture of the resistivity distribution in the plane of the section. The principles of the technique were shown in figure (2.25).

The pseudosection is made to present raw data, and is also a tool for rapid visual assessment of data quality. Large inconsistent changes between adjacent data points in the pseudosection, is often a sign of bad data quality in the measurements. Adjacent data point involves to a great extent the same subsurface volume for the measurement and their respective potential readings should therefore vary in a systematic way. Slight errors in data will not be identified by checking the pseudosection, but obviously incorrect data points resulting from for instance instrumentation errors, failure of the relays in the switching unit, shorting of the cables in wet conditions, or mistakes during field surveying may be identified. It is essential to remove such obviously incorrect data points before moving on to the next step in achieving a final resistivity model, the inverse modeling.

Pseudosection reflects qualitatively the spatial variation in resistivity in the vertical cross-section (Griffiths and Turnbull, 1985). The unit electrode spacing determines the length of the profile, depth of investigation and resolution.

Because we intend to use RES2DINV program, we restricted to describe the forward modeling algorithm and inversion subroutines which is used in this program.

Forward modeling

The contoured data can be modeled using a two-dimensional (2D) finite element or finite difference algorithm (Dey and Morrison, 1979) to calculate the 2-D forward response of the model.

In 2D forward modeling the subsurface resistivity distribution is described by a 2D model extended in infinity in the third direction. It is important to notice, however, that the sources, the current electrodes, are modeled as 3D sources. If not, they would obviously be mistakenly described as line electrodes.

The forward modeling finds a solution to the current flow equations in inhomogeneous ground for a given resistivity distribution and current source configuration. The solution includes the potential field in the investigated 2D section, from which calculation of the apparent resistivities from the configuration of the potential electrodes are straightforward.

The simplified equation for 2D is typically solved numerically by dividing the subsurface in a number of finite elements and solves by matrix inversion techniques. The most common numerical methods are the finite differences or the finite element method. The method of finite differences has been used as default except for when topography is included then the finite element method is preferred due to more flexibility in arranging the cells.

Inversion Method

In the automatic inversion routine a homogeneous starting model of the subsurface resistivity distribution is used with logarithmic averages of the measured apparent resistivities (Loke and Barker, 1995). The subsurface is divided into a large number of rectangular cells, and the optimization method attempts to determine the resistivity distribution of the cells that minimizes the difference between the calculated and measured apparent values subject to certain constraints (Loke *et al.*, 2003).

The regularized least-squares optimization method is a flexible technique that can be modified by using constraints that agree more closely with the true geology. By using the proper constraints, significant improvements in the resulting model can be obtained. This method is widely used in 2D and 3D resistivity inversion as it usually leads to a stable solution. It gives results that closely correspond to the true geology in situations where the resistivity changes in a gradual and smooth manner. However, in situations with sharp boundaries, the results are not optimal.

Loke and Barker (1995) described a fast technique based on the least-squares optimization method that requires only a modest amount of computing time. It produces a model that is free of distortions in the original apparent resistivity pseudosection caused by the electrode array geometry. It is also relatively insensitive to random noise in the data. They called this technique the "least-squares deconvolution method" because it separates the effect of the electrode array geometry on the apparent resistivity values from that which results from the subsurface resistivity.

Loke and Barker (1996a) used an inversion model where the arrangement of the model blocks directly follows the arrangement of the pseudosection plotting points. This approach gives satisfactory results for the Wenner and Wenner-Schlumberger arrays where the pseudosection point falls in an area with high sensitivity values. However, it is not suitable for arrays such as the dipole-dipole and pole-dipole where the pseudosection point falls in an area with very low sensitivity values. The RES2DINV program uses a more sophisticated method to generate the inversion model where the arrangement of the model blocks is not tightly bound to the pseudosection.

Loke and Dahlin (1997) found a method which combines the accuracy of the Gauss-Newton method (deGroot-Hedlin and Constable, 1990; Sasaki, 1994) with the speed of the quasi-Newton method (Loke and Barker, 1996 a,b).

The least-squares formulation, which constrains the smoothness of the model parameters to a constant value, is given by the following equation:

$$\left(J_i^T J_i + d_i C^T C\right) p_i = J_i^T g_i - \lambda_i C^T C r_{i-1} \ldots\ldots \text{(24)}$$

where (J_i) is the Jacobian matrix of partial derivatives, (C) is the flatness filter matrix, (g_i) is a vector which contains the differences between the logarithms of the measured and calculated apparent resistivity values, (d_i) is the damping factor, (p_i) is the perturbation vector to the model parameters for the *i*th iteration, and (r_{i-1}) is the model parameters vector for the previous iteration.

This method recalculating the partial derivatives for the first 2 or 3 iterations represents a good compromise between reducing the computing time and obtaining sufficiently accurate results. The computer time is reduced by about h which is particularly important in 3D resistivity inversion which can involve more than 10000 datum and very large finite-difference grids.

For 3D resistivity imaging, the inversion program divides the subsurface into a number of small rectangular prisms, and attempts to determine the resistivity values of the prisms so as to minimize the difference between the calculated and observed apparent resistivity values. One possible arrangement used by Loke and Barker (1996b) is shown in figure (2.26).

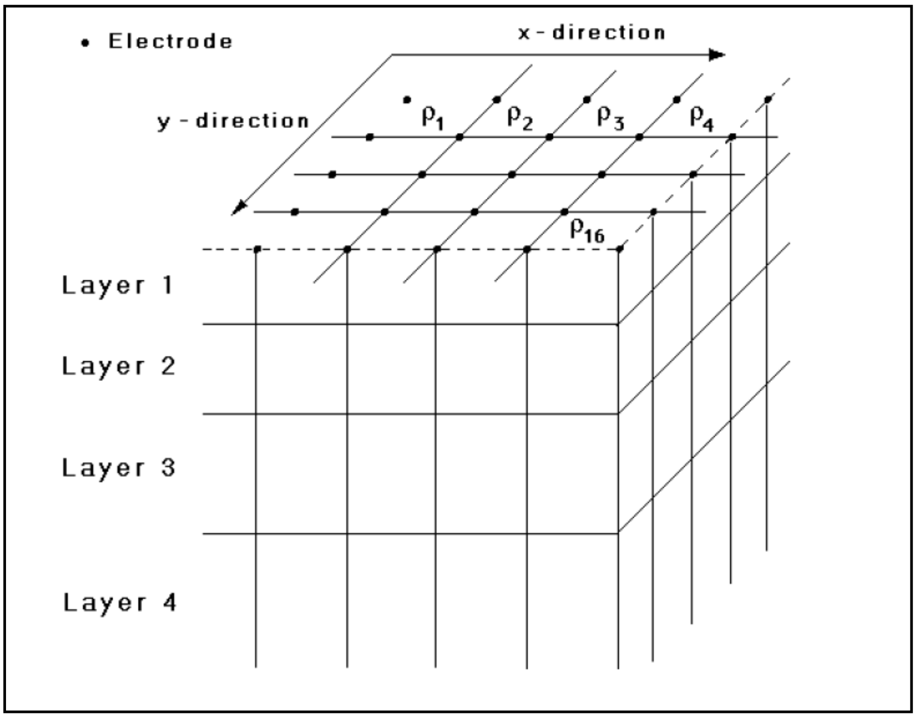

Figure (2.26) The model blocks arrangement used by (Loke and Barker, 1996b).

The optimization method tries to reduce the difference between the calculated and measured apparent resistivity values by adjusting the resistivity of the model blocks

The inversion routine is based on the smoothness constrained least-squares method (deGroot-Hedlin and Constable, 1990; Sasaki, 1992; Loke and Barker, 1996a).

The inversion procedure of measured data (for 2D and3D imaging) can be summarized in a flow chart as in figure (2.27).

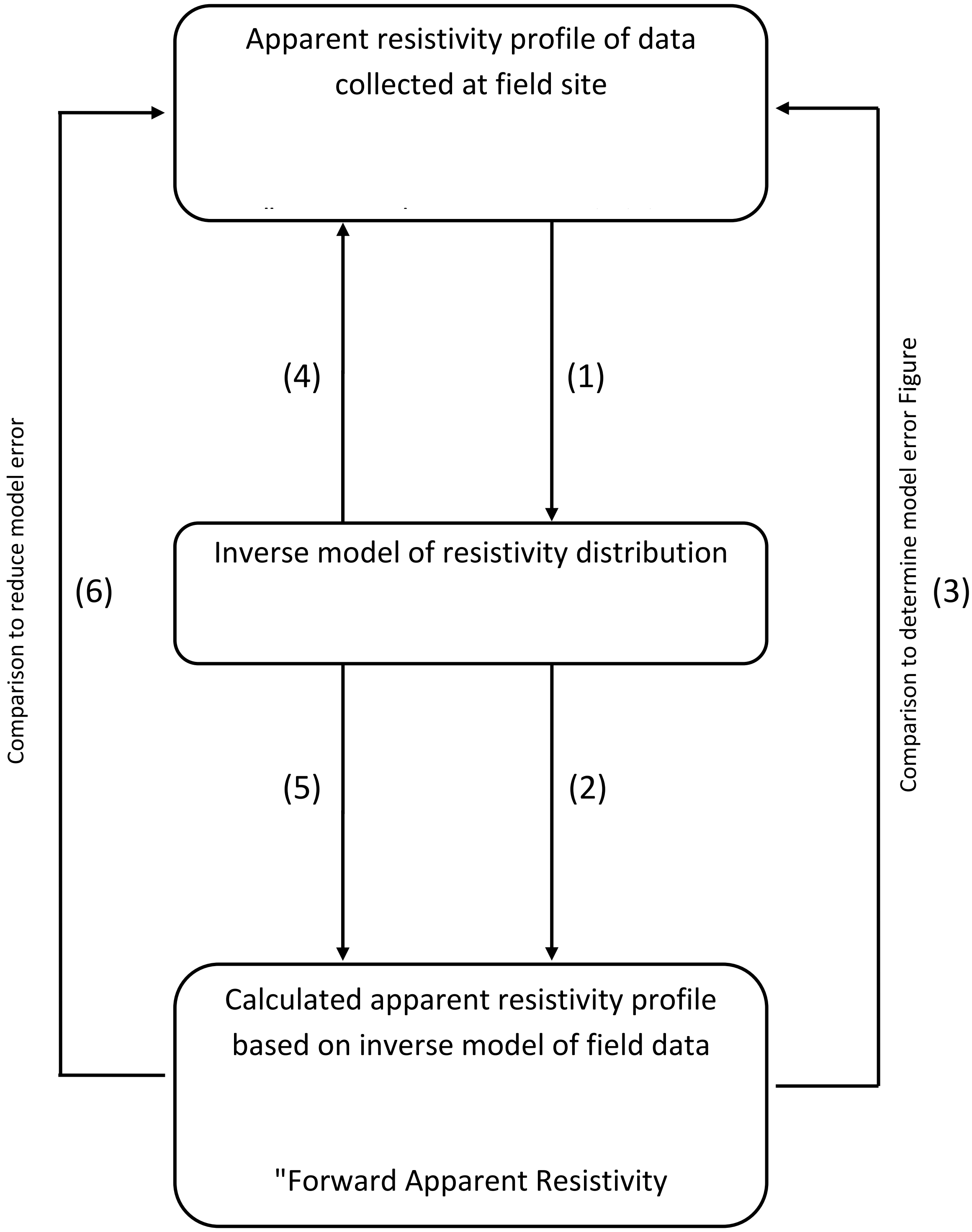

Figure (2.27) Overview of resistivity imaging inversion process.

Processing steps in figure (2.27) are as following:

1. Measured apparent resistivity data from field site are imported, and an apparent resistivity profile for the measured data is generated.
2. A calculated apparent resistivity profile for the inverted model is generated.
3. The two apparent resistivity profiles are compared to determine the root mean square (RMS) error between them.

Steps 1, 2 and 3 are representing the forward modeling.

4. Modifying the inverted resistivity model according to the measured field data.
5. Generating a new calculated apparent resistivity for the inverted model.
6. Comparing the new calculated apparent resistivity profile with the measured apparent resistivity profile to reduce the root mean square (RMS) error between them.

Steps 4, 5 and 6 are representing the inversion process, and they all done in the first iteration. The iteration is repeated, decreasing the RMS error until it meets a user-defined value or the number of iterations reaches a user-defined maximum.

Data interpretation

For interpretation of a final 2D inverted resistivity model it is wise to always keep in mind some typical phenomena associated with the theories behind resistivity measurements that may affect the final model. A few such factors are listed below (Sjodahl, 2006):

- Depth resolution: The resolving power of the resistivity method decreases exponentially with depth.
- Resolution at the sides of the model: At the sides of the final model there are less data points and the model may be strongly affected by boundary conditions and the weight the side blocks are assigned in the inversion. In many cases this problem can be overcome by increasing the length of the survey line so that the area of interest surely becomes entirely covered.

- The concept of non-uniqueness: The principle of equivalence can be exemplified for the case of a homogeneous earth with an embedded horizontal high-resistive layer. In that situation the high-resistive layer with a certain resistivity and a certain thickness may, within the measurement resolution, produce the same result as a layer with twice the resistivity and half the thickness (Telford, 1990).
- High-resistive or high-conductive top layer: If the top layer is very resistive it might be difficult to get enough current into the ground. On the other hand, if the top layer is very conductive the current will be channeled into this layer and it might be difficult to reach the underlying structures with enough current. In both cases, the potential readings may become very small resulting in very low signal-to-noise ratios.
- 3D effects: Inversion of 2D resistivity data assumes a 2D subsurface reality and no significant variations in the direction perpendicular to the survey line. This is rarely the case, but for many surveys it is a manageable problem. A four-electrode measurement involves an earth volume with the shape of a half-sphere for the case of a homogeneous subsurface. This means in principle that structures on a certain distance to the side of the line has the same influence on the measurements as structures on a similar depth.

Hydrocarbon detection

Field studies of oil pollution are more difficult in the case of high ground water salinity, as the resistivity contrast between soils with and without pollutants is minimal (Ryjov and Shevnin, 2002).

Difference of lithology establishes a background resistivity range of the medium, from highly resistive rocks like limestone, to highly conductive ones like clay. Thus oil pollution also depends on lithology.

The ground water level position is another important factor. Depending on salt concentration in the water, resistivity of saturated rocks varies considerably. Besides, the pollutants change the electrical characteristics of rocks above and below groundwater level.

A model of oil pollution has the following features: rapid changes of electrical properties in time in comparison with natural geological processes; migration in space together with groundwater flow; migration at depth across the groundwater level; diminishing groundwater resistivity (up to 5 times in sands and up to 50 times in pore space of clays); structural control of contamination by faults, and lithological control.

Hydrocarbons may become visible to conventional DC electrical resistivity and electromagnetic induction conductivity mapping when the hydrocarbon preferentially wets the soil, significantly decreasing the electrical conductivity of the porous system (Waxman and Thomas, 1974). Without the preferential wetting (most common in carbonates), the thin film of water wetting the soil surfaces remains as a continuous connected current pathway, so electrical conductivity changes are very slight, even with significant amounts of contaminant (Sadowski, 1988). The presence of the insulating hydrocarbon layer floating on the water table has also been modeled to produce a shadowing or screening effect on electrical measurements (Mazac *et al.*, 1990). Hydrocarbons may also produce an electrical conductivity increase (Andres and Canace, 1984), oil contamination of soil, after four months to one year after contamination, creates a low resistivity zone (Sauck, 1998; 2000), even though an insulating material is being added, when the entrance of the hydrocarbon causes a flushing of salts from the soil surfaces, resulting in a briny halo around the hydrocarbon. Also, TDS and bulk conductivities of sediments found to be generally higher at locations contaminated with hydrocarbon and undergoing intrinsic biodegradation; biodegradation processes can impact both electrolytic and surface conduction properties of contaminated sediments and these two factors can account for the higher bulk conductivities observed in sediments impacted by hydrocarbon (Atekwana *et al.*, 2004).

The problem in relying on measurements of electrical conductivity changes to detect hydrocarbons is that the electrical conductivity may increase, decrease or hardly change depending upon site specific conditions, or the change in electrical conductivity due to the presence of the hydrocarbons may be negligible in comparison to other changes at the site such as varying depth to water table (Olhoeft, 1986).

References

AL-Menshed, F.H, 2011. Evaluation of resistivity method in delineation ground water hydrocarbon contamination southwest of Karbala city. Unpublished, PhD thesis. University of Baghdad, college of science